Magnetic field effect on the cross section of Higgs boson production through gluon fusion

Jorge Igor Jaber-Urquiza[1]

Facultad de Ciencias - UNAM

In collaboration with: Angel Sánchez

Workshop on Electromagnetic Effects in Strongly Interacting Matter

ICTP-SAIFR, São Paulo, Brazil

October 25-28, 2022.

[1] jorgejaber@ciencias.unam.mx

Overview

A brief insight

- Higgs field is responsible for generating the masses of the elementary particles of the SM through the electroweak SSB.
- Precisely characterizing the properties of the Higgs boson would help us better understand the nature of electroweak SSB[2], Yukawa's couplings[3], etc.
- Theoretically, very precise calculations of the Higgs boson properties, such as its production and decay modes by different channels, have been elaborated[4].
- The production of Higgs bosons by gluon fusion is a process of great relevance because it corresponds up to 87% of the production at 14 TeV[5].

[2] M. Bier *et al.* *JHEP* **01**, 164, (2014).
[3] A. M. Sirunyan *et al.* *Phys. Lett.* B **778**, 101, (2018).
[4] A. Sopczak *et al.* *PoS(FFK2019)*, 006, (2019).
[5] R. Workman *et al.* (PDG), *Prog. Theor. Exp. Phys.* 2022, 083C01 (2022).

Higgs beyond proton-proton collision

So far, the research referred has focused only on the physics of the Higgs boson in vacuum (proton-proton collisions).

Recent studies show the possibility of the production/detection of Higgs bosons in other types of collisions; for example, in relativistic heavy ion collisions[6].

Depending on the stage of the Higgs boson formation and decay, the effects of "glasma" and/or QGP would have to be considered.

- Presence of a magnetic field[7].
- Temperature.

[6] E. L. Berger *et al. Phys. Rev. Lett.* **122**, 041803, (2019).
D. d'Enterria *et al. Phys. Rev.* D **101**, 033009, (2020).

[7] D. E. Kharzeev *et al. Nucl. Phys.* A **803**, 227, (2008).

Magnetic fields in peripheral relativistic heavy ion collisions

- Very intense at the beginning ($\sim m_\pi^2$) and decay exponentially with a characteristic time of $\sim$fm/c[8].

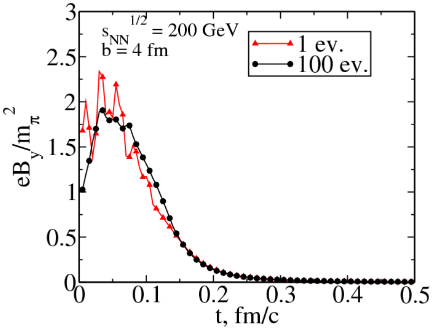

Figure: The time evolution of the magnetic field strength eB_y at the central point O in Au-Au collisions with impact parameter $b = 4$fm in the UrQMD model, in one event ("1ev") and and averaged over 100 events ("100ev"). The symbols are plotted every $\Delta t = 0.2$fm/c for $E_{\rm lab} = 60$GeV and $\Delta t = 0.01$fm/c for $\sqrt{S_{NN}} = 200$GeV.

[8] V. V. Skokov *et al.* *Nucl. Phys.* A **24**, 708, (2009).

Higgs boson production through gluon fusion

The Higgs boson production through gluon fusion process

$$gg \longrightarrow H,$$

is described by the amplitude

$$M^{\mu\nu} = \langle p_H; + | (p_1, \mu, \lambda_1), (p_2, \nu, \lambda_2); - \rangle \,.$$

There is not a direct interaction between gluons and the Higgs boson, so the contributions to the process come from radiative corrections.

At leading order, there are two different contributions to the amplitude, i.e., two Feynman diagrams.

Effective vertex

Since this amplitude represents a direct interaction among three particles, as shown schematically in the figure below, from now on we shall treat this as an effective vertex, named $\Gamma^{\mu\nu}$.

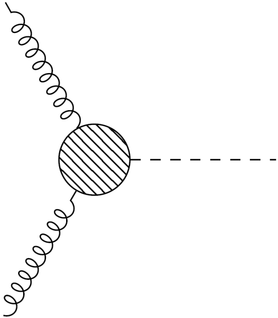

Higgs boson production through gluon fusion in presence of an external magnetic field

The two different contributions to the amplitude at leading order are represented by the Feynman diagrams

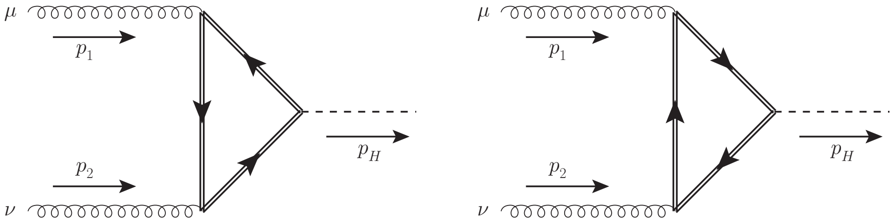

(a) Diagram A. (b) Diagram B.

Figure: Feynman diagrams at leading order process in the presence of an external magnetic field. The magnetic field is represented by a double line in the fermionic propagators.

Magnetic field vertex structure

An external magnetic field generates a more diverse structure in comparison with the vacuum case[9]

$$p_j^\mu,\ F^{\mu\nu}p_{j\nu},\ F^{\mu}{}_{\alpha}F^{\alpha\nu}p_{j\nu}\ \&\ F^{*\mu\nu}p_{j\nu},$$

with $j = 1, 2$ and $F^{\mu\nu}$ the electromagnetic tensor.

The magnetic field rises to eight the linear independent four-vectors that we have at our disposal.

This generate new rank two tensor structures that have to be included in the effective vertex.

[9] I. Batalin and A. Shabad, *Zh. Eksp. Teor. Fiz.* **60**, 894, (1971).

The polarization vectors of a gluon with momentum p_1^μ can be expanded in the following four independent vectors[10]

$$
\begin{aligned}
l_1^\mu &\equiv p_1^\mu, \\
L_1^\mu &\equiv \hat{F}^{\mu\nu} p_{1\nu}, \\
L_1^{*\mu} &\equiv \hat{F}^{*\mu\nu} p_{1\nu}, \\
G_1^\mu &\equiv \frac{l_1^2}{L_1^2} \hat{F}^{\mu\alpha} \hat{F}_{\alpha\beta} p_1^\beta + l_1^\mu .
\end{aligned}
$$

This polarization vector basis satisfies the completeness relation

$$
g^{\mu\nu} = \frac{l_1^\mu l_1^\nu}{l_1^2} + \frac{L_1^\mu L_1^\nu}{L_1^2} + \frac{L_1^{*\mu} L_1^{*\nu}}{L_1^{*2}} + \frac{G_1^\mu G_1^\nu}{G_1^2}.
$$

[10] I. Batalin and A. Shabad, *Zh. Eksp. Teor. Fiz.* **60**, 894, (1971).
V. I. Ritus, *Annals of Physics* **69**, 555, (1972).

How does the effective vertex looks like?

Working with these two basis will be advantageous because each gluon can be described with their respective polarization vectors.

Therefore, the most general structure for the effective vertex in presence of an external magnetic field is given by[11]

$$\begin{aligned}\Gamma^{\mu\nu}_{qB}(p_1,p_2) =& a_1\frac{L_1^\mu L_2^\nu}{|L_1||L_2|} + a_2\frac{L_1^{*\mu} L_2^{*\nu}}{|L_1^*||L_2^*|} + a_3\frac{G_1^\mu G_2^\nu}{|G_1||G_2|} + a_4\frac{L_1^\mu L_2^{*\nu}}{|L_1||L_2^*|}\\ &+ a_5\frac{L_1^{*\mu} L_2^\nu}{|L_1^*||L_2|} + a_6\frac{L_1^\mu G_2^\nu}{|L_1||G_2|} + a_7\frac{G_1^\mu L_2^\nu}{|G_1||L_2|} + a_8\frac{L_1^{*\mu} G_2^\nu}{|L_1^*||G_2|} + a_9\frac{G_1^\mu L_2^{*\nu}}{|G_1||L_2^*|}.\end{aligned}$$

[11] V. O. Papanyan and I. Ritus, *Zh. Eksp. Teor. Fiz.* **61**, 2231, (1972) & *Zh. Eksp. Teor. Fiz.* **65**, 1756, (1973).

Effective vertex proprieties

- Generalized Ward identities

$$p_1^\mu \Gamma_{\mu\nu}(p_1, p_2) = 0,$$
$$p_2^\nu \Gamma_{\mu\nu}(p_1, p_2) = 0.$$

- Bosonic exchange

$$\Gamma^{\mu\nu}(p_1, p_2) = \Gamma^{\nu\mu}(p_2, p_1).$$

- Invariance under charge conjugation (C) and parity (P).

Taking into account all the above proprieties and working with on-shell gluons, the final form for the effective vertex, in presence of an external magnetic field, is given by

$$\Gamma^{\mu\nu}_{qB}(p_1,p_2) = a_1^{++}\frac{L_1^\mu L_2^\nu}{|L_1||L_2|} + a_2^{++}\frac{L_1^{*\mu}L_2^{*\nu}}{|L_1^*||L_2^*|} + a_4^{-+}\left(\frac{L_1^\mu L_2^{*\nu}}{|L_1||L_2^*|} + \frac{L_1^{*\mu}L_2^\nu}{|L_1^*||L_2|}\right),$$

where the notation $a_i^{P,C}$ indicates its behavior under Parity and Charge transformations, respectively.

Note: a gluon can be only in three polarization states L^μ, $L^{*\mu}$ and G^μ. In the case of an on-shell gluon, there are only two polarization sates because the dispersion relation $l^2 = 0$, reduces G^μ to l^μ.

Cross section

The unpolarized cross section for the process is given by

$$\sigma\left(gg \longrightarrow H\right) = \frac{1}{2m_H^2}\int \frac{d^3p_H}{(2\pi)^3 2E_H}(2\pi)^4\delta^{(4)}\left(p_1+p_2-p_H\right)\overline{\sum}_{\text{color, spin}}|\mathcal{M}|^2$$
$$= \frac{1}{2m_H^2}2\pi\delta\left(\mathcal{S}-m_H^2\right)\overline{\sum}_{\text{color, spin}}|\mathcal{M}|^2,$$

with

$$i\mathcal{M} = i\Gamma^{\mu\nu}(p_1,p_2)\epsilon_\mu^a(p_1,\lambda_1)\epsilon_\nu^b(p_2,\lambda_2).$$

Cross section

The unpolarized cross section for the process is given by

$$\sigma\left(gg \longrightarrow H\right) = \frac{1}{2m_H^2}\int \frac{d^3p_H}{(2\pi)^3 2E_H}(2\pi)^4\delta^{(4)}\left(p_1+p_2-p_H\right)\overline{\sum}_{\text{color, spin}}|\mathcal{M}|^2$$
$$= \frac{1}{2m_H^2}2\pi\delta\left(\mathcal{S}-m_H^2\right)\overline{\sum}_{\text{color, spin}}|\mathcal{M}|^2,$$

with

$$i\mathcal{M} = i\Gamma^{\mu\nu}(p_1,p_2)\epsilon_\mu^a(p_1,\lambda_1)\epsilon_\nu^b(p_2,\lambda_2).$$

Finally, we obtain the expression

$$\sigma_{qB}\left(gg \longrightarrow H\right) = \frac{1}{256m_H^2}\left(|\tilde{a}_1|^2+|\tilde{a}_2|^2+2|\tilde{a}_4|^2\right)2\pi\delta\left(\mathcal{S}-m_H^2\right),$$

where the coefficients have been redefined by a color factor.

One-loop effective vertex in the presence of a magnetic field

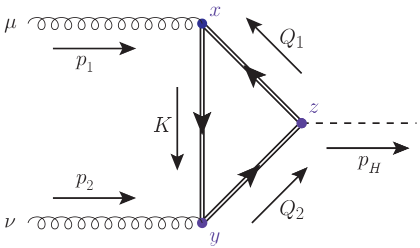

(a) Diagram A.

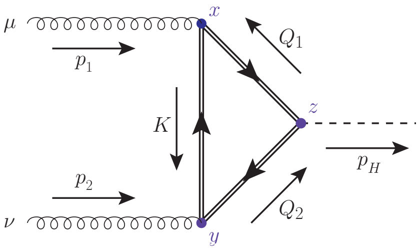

(b) Diagram B.

Figure: Feynman diagrams at leading order process in the presence of an external magnetic field. The internal/external arrows denote the charge/momentum flux.

Fermionic propagator in the presence of a magnetic field

The fermionic propagator in the presence of a magnetic field was obtained by Schwinger (in the configuration space) and is given by[12]

$$S^{qB}(x,y) = \Omega(x,y) \int \frac{d^4p}{(2\pi)^4} \tilde{S}^{qB}(p) e^{-ip\cdot(x-y)},$$

where

$$\Omega(x',x'') = \exp\left(-iq \int_{x''}^{x'} A_\mu(x) dx^\mu\right)$$

it's known as Schwinger phase, with q the electric charge of the fermion and A^μ the potential that generates the magnetic field $\vec{B}$.

[12] A. Erdas. *Phys. Rev.* D **82**, 664, (2009).

In the particular case of a homogeneous magnetic field that defines the direction z, the translationally invariant part of the fermionic propagator in moment space can be written in Schwinge's proper time representation as [13]

$$\tilde{S}^{qB}(p) = \int_0^\infty \frac{ds}{\cos(|qB|s)} \exp\left[-is\left(m^2 - p_\parallel^2 - p_\perp^2 \frac{\tan(|qB|s)}{|qB|s} \right) \right] \times \left[\left(m + \not{p}_\parallel \right) e^{\mathrm{sgn}(qB)i|qB|s\Sigma_3} + \frac{\not{p}_\perp}{\cos(|qB|s)} \right],$$

where $p_\parallel$ and $p_\perp$ are the parallel and perpendicular components of the momentum to the magnetic field, such that

$$p^2 = p_0^2 - p_x^2 - p_y^2 - p_z^2 \equiv p_\parallel^2 + p_\perp^2.$$

The spin matrix along the z-direction, reads

$$\Sigma_3 \equiv i\gamma^1\gamma^2.$$

[13] A. Erdas. *Phys. Rev.* D **82**, 664, (2009).

Applying the Feynman rules, we obtain the analytic expressions for the two contributions in configuration space

$$i\Gamma_{qB}{}^{\mu\nu}_{(A)}(x,y,z) = -\mathcal{TR}\left[\left(-ig_s\gamma^{\mu}t^{a}\right)S^{qB}(x,z)\left(-ig_{f}\right)S^{qB}(z,y)\left(-ig_s\gamma^{\nu}t^{b}\right)S^{qB}(y,x)\right]$$

and

$$i\Gamma_{qB}{}^{\mu\nu}_{(B)}(x,y,z) = -\mathcal{TR}\left[\left(-ig_s\gamma^{\mu}t^{a}\right)S^{qB}(x,y)\left(-ig_s\gamma^{\nu}t^{b}\right)S^{qB}(y,z)\left(-ig_{f}\right)S^{qB}(z,x)\right].$$

Applying the Feynman rules, we obtain the analytic expressions for the two contributions in configuration space

$$
\begin{aligned}
i\Gamma_{qB}{}^{\mu\nu}_{(A)}(x,y,z) &= -\mathcal{TR}\left[\left(-ig_s\gamma^{\mu}t^{a}\right) S^{qB}(x,z)\left(-ig_f\right) S^{qB}(z,y)\left(-ig_s\gamma^{\nu}t^{b}\right) S^{qB}(y,x)\right]\\
&= -ig_s^2 g_f \,\mathrm{tr}\left[t^a t^b\right]\Omega(x,z)\Omega(z,y)\Omega(y,x)\\
&\qquad\times\int\frac{d^4K\ d^4Q_1\ d^4Q_2}{(2\pi)^4(2\pi)^4(2\pi)^4}e^{-iK\cdot(y-x)}e^{-iQ_1\cdot(x-z)}e^{-iQ_2\cdot(z-y)}\\
&\qquad\qquad\times Tr\left[\gamma^{\mu}\tilde{S}^{qB}(Q_1)\tilde{S}^{qB}(Q_2)\gamma^{\nu}\tilde{S}^{qB}(K)\right],
\end{aligned}
$$

and

$$
i\Gamma_{qB}{}^{\mu\nu}_{(B)}(x,y,z) = -\mathcal{TR}\left[\left(-ig_s\gamma^{\mu}t^{a}\right) S^{qB}(x,y)\left(-ig_s\gamma^{\nu}t^{b}\right) S^{qB}(y,z)\left(-ig_f\right) S^{qB}(z,x)\right].
$$

Summary on the integration process

In order to obtain an expression for the effective vertex in the space of moments it is necessary to

- Carry out the integration over the configuration space

$$\Gamma_{qB}{}^{\mu\nu}(p_1,p_2,p_H) = \int d^D x \; d^D y \; d^D z \; \Gamma_{qB}{}^{\mu\nu}(x,y,z) e^{-ip_1\cdot x} e^{-ip_2\cdot y} e^{+ip_H\cdot z}.$$

  - Generalization to D dimensions.
  - Schwinger's phases play an important role.
  - The phase associated with each diagram is opposite.

- Carry out the integration over the loop momenta.
  - Do not calculate the spinorial trace.
  - Gaussian integrals with "shift".

What's next?

- Compute the integrals on the Schwinger's parameters, s_i.
- Calculate the spinorial trace.
- Project on the basis of Ritus to obtain the coefficients that contribute to the cross section

$$
\begin{aligned}
a_1 &= {\Gamma_{qB}}^{\mu\nu} \frac{L_{1\mu} L_{2\nu}}{|L_1||L_2|}, \\
a_2 &= {\Gamma_{qB}}^{\mu\nu} \frac{L^*_{1\mu} L^*_{2\nu}}{|L^*_1||L^*_2|}, \\
a_4 &= {\Gamma_{qB}}^{\mu\nu} \frac{L_{1\mu} L^*_{2\nu}}{|L_1||L^*_2|} = {\Gamma_{qB}}^{\mu\nu} \frac{L^*_{1\mu} L_{2\nu}}{|L^*_1||L_2|}.
\end{aligned}
$$

Approximations

The integrals that remain to be solved over the s_i parameters cannot be calculated analytically, so it is necessary perform out certain approximations.

The most frequently used approaches in the literature are

- Weak magnetic field.
- Strong magnetic field.

These approximations are taken when $|qB| \ll m_f^2$ and $|qB| \gg m_f^2$, respectively[14].

[14] To get a reference, the critical magnetic field for a electron is $4.4 \times 10^{13}\text{G} \sim (0.5MeV)^2$

Weak field approximation with low transverse momentum

For now, let us restrict ourselves to work with a weak field approximation, $|qB| \ll m_f^2$ (ideal for heavy quarks). With this in mind, it's possible to perform a Taylor expansion on the various functions that contain qB terms in their argument.

The remaining physical scales (the gluon momenta) also play an important role and must be considered in any approximation

$$\exp\left[-\frac{i}{|qB|}\frac{\mathbf{t_1 t_3}p_{1\perp}^2 + \mathbf{t_2 t_3}p_{2\perp}^2 + \mathbf{t_1 t_3}q_\perp^2 \pm 2\mathbf{t_1 t_2 t_3}p_2\hat{F}p_1}{\mathbf{t_1 t_2 t_3} - \mathbf{t_1} - \mathbf{t_2} - \mathbf{t}an\left(|qB|s_3\right)}\right].$$

Let's see the results obtained with this approximation for the cross section in the presence of an external magnetic field and compare it with the vacuum case.

Magnetic field on the cross section

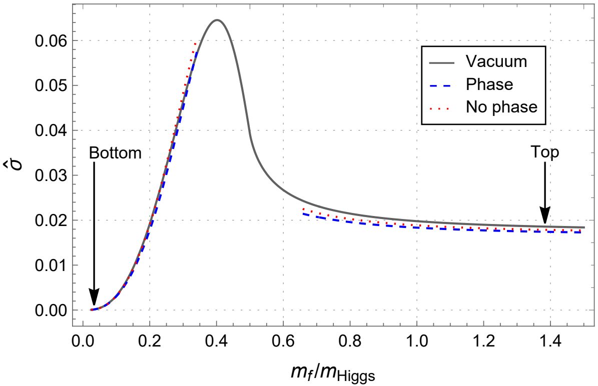

Figure: Behavior of the cross section as a function of the mass of the quarks inside the loop for a head to head gluon fusion with $|qB| = 0.1m_f^2$. The Higgs bosons are produced at rest and the kinematic parameters are given by $\Theta = \pi$, $|p_{i_\perp}| = 0.3m_f$ and $|p_{i_z}| = \frac{1}{2}\sqrt{m_H^2 - 4(0.3m_f)^2}$.

System response

In order to highlight the effects coming from the magnetic field and the gluon transverse momenta, it is convenient to define the "system response" as

$$\Delta\sigma \equiv \frac{\sigma_{qB} - \sigma_{\text{vacuum}}}{\sigma_{\text{vacuum}}}.$$

Phase effect

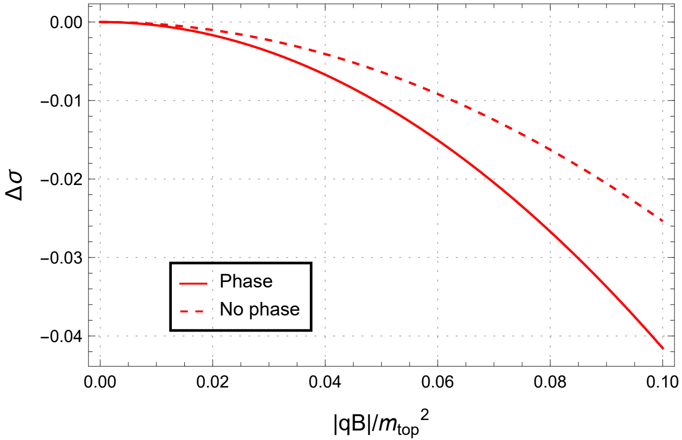

Figure: Phase effect on the system response for the top quark as a function of magnetic field strength for a frontal gluon fusion fully contained in the transverse plane. The Higgs bosons are produced at rest and the kinematic parameters are given by $\Theta = \pi$, $|p_{i\perp}| = 0.361 m_{top}$ and $|p_{i_z}| = 0$.

Head to head gluon fusion in the $\perp$ plane

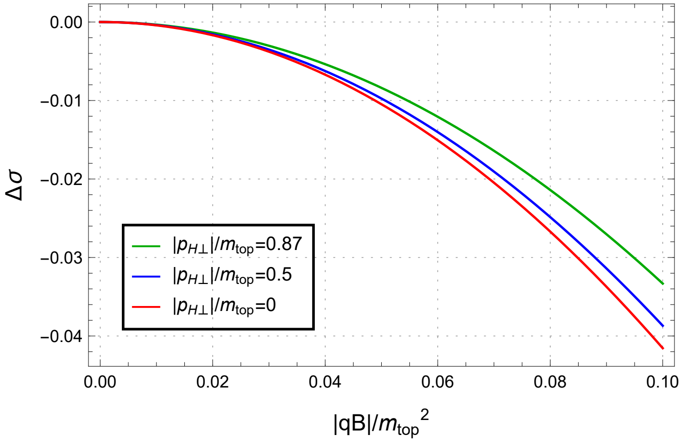

Figure: System response for a frontal gluon fusion fully contained in the transverse plane as a function of the magnetic field strength. The Higgs bosons are produced over the fusion line with different transverse momentum and the rest of kinematic parameters are given by $\Theta = \pi$ and $|p_{i_z}| = 0$.

Orientation of the processes respect to $\vec{B}$

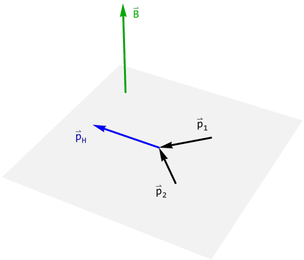

(a) Perpendicular pure.

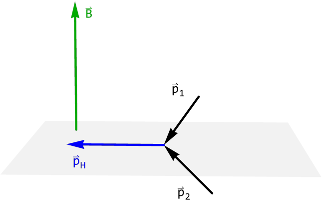

(b) Perpendicular mixed.

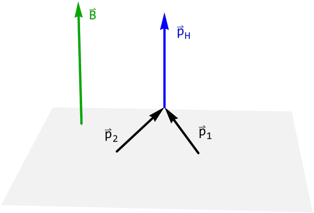

(c) Parallel mixed.

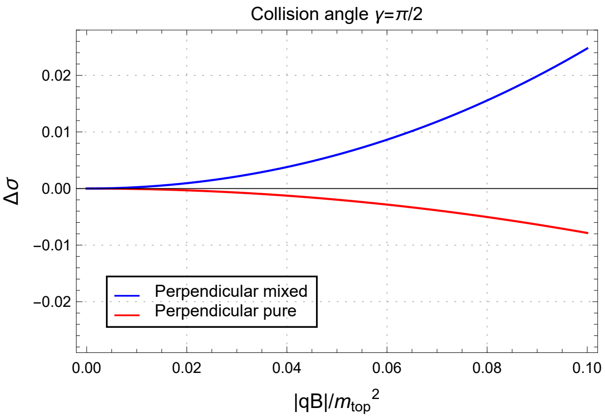

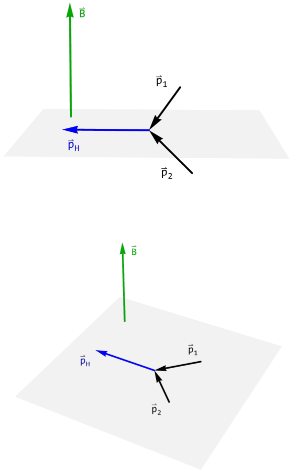

Figure: Comparison of the system response as a function of magnetic field strength for the perpendicular mixed and perpendicular pure configurations of the process with collision angle $\gamma = \pi/2$ and $|\vec{p}_i| = m_H/\sqrt{2}$.

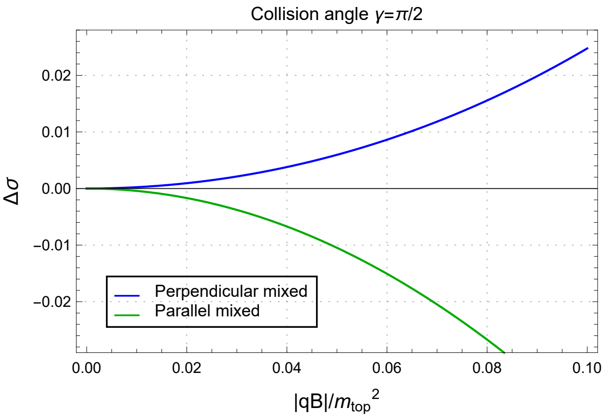

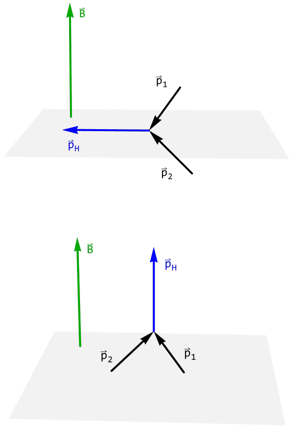

Figure: Comparison of the system response as a function of magnetic field strength for the perpendicular mixed and parallel mixed configurations of the process with a collision angle of $\gamma = \pi/2$ and $|\vec{p}_i| = m_H/\sqrt{2}$.

Final remarks

- Polarization states basis is a very useful tool to find the structure for general processes that involve vector bosons.
- The methodology used in this work allow us to compute exact (without any approximations) and compact analytical expressions.
- Schwinger phase plays a role in the process. In this case, tends to reduce the effect of the magnetic field but does not change the tendency.
- For head to head gluon fusion, fully contained in the perpendicular plane, the presence of the magnetic field reduces the cross section meanwhile the perpendicular momentum has the opposite effect.
- The cross section, as a function of $|qB|$, exhibits an angular dependence Θ. This is, the incident gluons orientations (respect to $\vec{B}$) is relevant.
- The Higgs production along the z axis decreases in presence of the magnetic field meanwhile the production in the perpendicular plane is more involved with the incident gluon orientation.

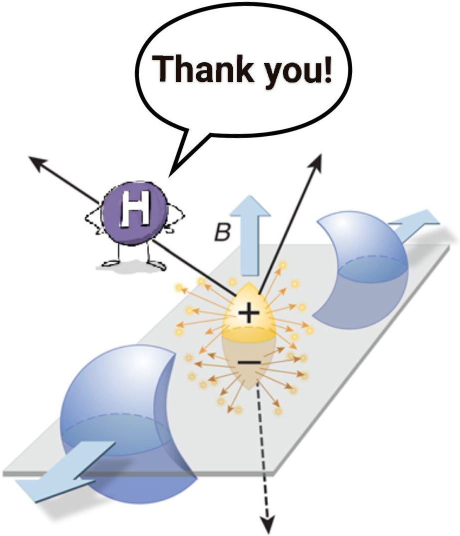
Thank you!
H
B
+
−

Work in progress

- Extend the analysis to the region of high perpendicular momenta, $|p_{i\perp}| \gg m_f$.
- To work with the light quarks, we need to work with an intense magnetic field approximation, $|qB| \gg m_f^2$.
- In order to work in an arbitrary magnetic field intensity $|qB|$, we need to develop a way to compute the integrals over Schwinger parameters in Eq. (26) numerically.
- To determine the effects on the total amount of Higgs produced ("directions" with increased or decreased production), the gluon distribution function of the RHIC have to be considered.

Why is Higgs boson so important?

- Higgs field is responsible for generating the masses of the elementary particles of the Standard Model (SM).
- This occurs through the spontaneous breaking of the electroweak symmetry.
- Since the confirmation of its existence in 2012, studying its properties became the main objective of the Higgs physics program.
- Precisely characterizing the properties of the Higgs boson would help us better understand the nature of spontaneous breaking of electroweak symmetry[15], Yukawa's couplings[16], etc.

[15] M. Bier *et al.* *JHEP* **01**, 164, (2014).
[16] A. M. Sirunyan *et al.* *Phys. Lett.* B **778**, 101, (2018).

Higgs production through gluon fusion

- The contribution to this process due to pure QCD interactions is around 95% while QCD-electroweak (QCD-EW) interactions contribute approximately 5%[17].
- "Leading-order" (LO) [18]
- "Next-to-leading-order" (NLO) $\sim 80 - 100\%$[19]
- "Next-to-next-to-leading-order" (NNLO or N^2LO) $\sim 10 - 20\%$[20]
- "Next-to-next-to-next-to-leading order" (N^3LO) $\sim 4 - 6\%$[21]

[17] M. Tanabashi *et al.* Phys. Rev. D **98**, 03001, (2018).
[18] H. M. Georgi *et al.* *Phys. Rev. Lett.* **40**, 692, (1978).
[19] M. Spira *et al.* *Phys. Lett.* B **453**, 17, (1995).
[20] C. Anastasious. *Nucl. Phys.* B **646**, 220, (2002).
[21] C. Anastasious *et al.* *JHEP* **05**, 058, (2016).

Cross section

- Theoretically, very precise calculations of the properties of the Higgs boson, such as its production and decay modes by different channels, have been elaborated[22].
- The cross section of Higgs production by different channels are physical observables that can be used for comparisons between the experimental and theoretical parts.
- It is possible to obtain information of the coupling constants, so it is a very useful tool to search for deviations in the SM predictions.
- The production of Higgs bosons by gluon fusion is a process of great relevance because it corresponds up to 87% of the production at 14 TeV[23].

[22] A. Sopczak *et al.* *PoS(FFK2019)*, 006, (2019).
[23] R. Workman *et al.* (PDG), *Prog. Theor. Exp. Phys.* 2022, 083C01 (2022).

External agents

- So far, the research referred has focused only on the physics of the Higgs boson in vacuum (proton-proton collisions).
- Nevertheless, they can be extended to scenarios where the effects of external agents could change the global properties of the Higgs boson[24].
- It is important to quantify the effect of these external agents in perturbative calculations to have clarity on the effects caused by "new physics".

[24] G. Gamow. *Phys. Rev.* **70**, 572, (1946).

Higgs beyond proton-proton collision

Recent studies show the possibility of the production/detection of Higgs bosons in other types of collisions; for example, in relativistic heavy ion collisions[25].

- Depending on the stage of the Higgs boson formation and decay, the effects of "glassma" and/or QGP would have to be considered. As well as temperature, density and the presence of a magnetic field.[26].
- The effects of these agents on the Higgs boson properties could be taken into account in a high-precision physics program.

[25] E. L. Berger *et al.* *Phys. Rev. Lett.* **122**, 041803, (2019).
D. d'Enterria *et al.* *Phys. Rev.* D **101**, 033009, (2020).

[26] D. E. Kharzeev *et al.* *Nucl. Phys.* A **803**, 227, (2008).

Magnetic fields in peripheral relativistic heavy ion collisions

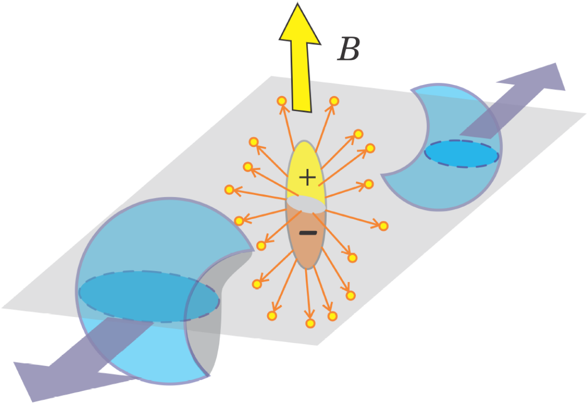

Figure: Sketch of a peripheral relativistic heavy ion collision.

Relativistic heavy ion collisions

In relativistic heavy ion collisions, it is possible to create an extreme high temperature and density environment that evolves over time[27]

- t=0 fm/c: In this initial stage the hadronic jets, direct photons, pairs of dileptons, heavy quarks, and vector bosons are produced.
- t$\sim$0.2 fm/c: A state called "glasma" is created, it's made up of non-equilibrium partonic matter at high density[28].
- t$\sim$1 fm/c: The partons that make up the "glasma" begin to interact strongly (QCD) with each other and a thermal equilibrium is reached.
- The result of this thermalization is a phase of QCD at high temperature known as "quark-gluon plasma" (QGP).

[27] E. Iancu. arXiv:1205.0579 [hep-ph].
[28] T. Lappi *et al.* *Nucl. Phys.* A **772**, 200, (2006).

Quark-gluon plasma

- The characteristic time for the expansion and cooling of the QGP is of the order of 10 fm/c[29].
- The mean lifetime of the Higgs boson is $\tau \sim 47$ fm/c[30].
- Taking this in consideration, we could imagine the following physical situations:
    - A Higgs boson produced in the initial stage of the collision (before the formation of the QGP) is affected by the plasma and modifies some of its properties such as the lifetime, the kinematic distribution, the decay rate, etc.
    - A Higgs boson is produced within the QGP, so that the main effect of the thermalized medium will be observed in the production rate.

[29] R. Shen *et al.* *Phys. Rev.* C **86**, 049903(E), (2012)
[30] M. Tanabashi *et al.* Phys. Rev. D **98**, 03001, (2018).

What else?

The Higgs field is described by a neutral scalar field, so the results of this research can be generalized and applied to various physical processes where a scalar field plays a central role.

- Inflation[31].
- Compact astrophysical objects (color superfluidity[32]).
- Production of different (pseudo)scalar particles in relativistic heavy ion collisions such as mesons (π, B, D), etc.

[31] T. Matos *et al.* *Classical Quantum Gravity* **17**, 1707, (2000)
[32] M. Alford *et al.* *Phys. Lett.* B **422**, 247, (1998).

Hierarchy of scales

Flavor	Electric charge $[e]$	$\lvert qB\rvert_{max}$ [GeV^2]
Up (u)	2/3	$\sim 10^{-6}$
Down (d)	-1/3	$\sim 4.4 \times 10^{-6}$
Strange (s)	-1/3	$\sim 2 \times 10^{-3}$
Charm (c)	2/3	~ 0.3
Bottom (b)	-1/3	~ 3.5
Top (t)	2/3	$\sim 6 \times 10^{3}$

Figure: Maximum magnetic field from which the weak field approximation loses validity, it's taken $|qB|_{max} = 0.2m_f^2$.

For a point of comparison, the maximum field that is created in relativistic heavy ion collisions is[34]

$$|eB|_{max} \simeq 10m_\pi^2 \sim 2 \times 10^4 \text{ MeV}^2 = 2 \times 10^{-2} \text{ GeV}^2.$$

[34] Y. Zhong et. al., *Advances in High Energy Physics*, **2014**, 193039, (2014).

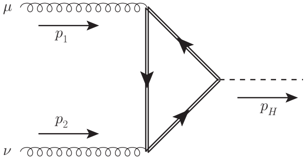

(a) Diagram A.

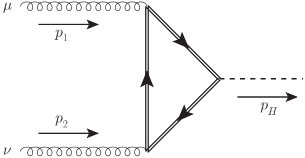

(b) Diagram B.

The effective vertex in the gluon polarization basis, in presence of an external magnetic field, is given by

$$\begin{aligned}\Gamma^{\mu\nu}_{qB}(p_1,p_2) =& a_1^{++}\frac{L_1^\mu L_2^\nu}{|L_1||L_2|}\\ &+ a_2^{++}\frac{L_1^{*\mu} L_2^{*\nu}}{|L_1^*||L_2^*|}\\ &+ a_4^{-+}\left(\frac{L_1^\mu L_2^{*\nu}}{|L_1||L_2^*|}+\frac{L_1^{*\mu} L_2^\nu}{|L_1^*||L_2|}\right),\end{aligned}$$

where the notation $a_i^{P,C}$ indicates its behavior under Parity and Charge transformations, respectively.

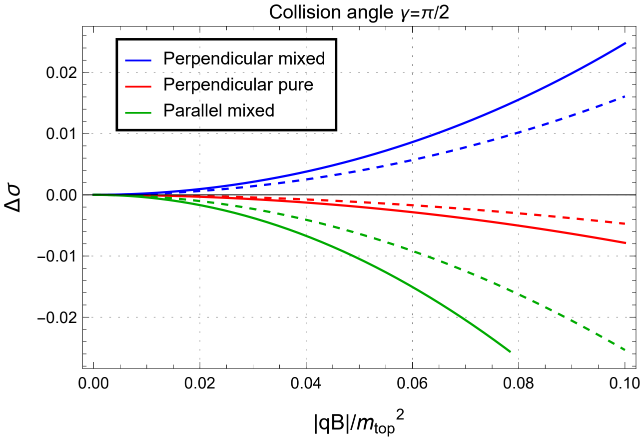

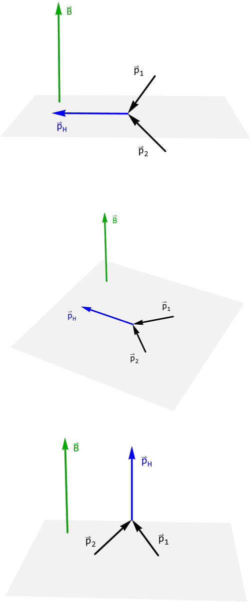

Figure: Comparison of the system response as a function of magnetic field strength for three different configurations of the process with collision angle $\gamma = \pi/2$ and $|\vec{p}_i| = m_H/\sqrt{2}$.